RESEARCH ARTICLE

Directional cues in *Drosophila melanogaster* audition: structure of acoustic flow and inter-antennal velocity differences

Erica L. Morley[1],*, Thomas Steinmann[2], Jérôme Casas[2] and Daniel Robert[1]

[1]School of Biological Sciences, University of Bristol, Woodland Road, Bristol BS8 1UG, UK and [2]Institut de Recherches sur la Biologie de l'Insecte, University of Tours, UMR CNRS 6035, 37200 Tours, France

*Author for correspondence (erica.morley@bristol.ac.uk)

SUMMARY

Drosophila melanogaster **have bilateral antisymmetric antennae that receive the particle velocity component of an acoustic stimulus. Acoustic communication is important in their courtship, which takes place in the acoustic near-field. Here, the small size of the dipole sound source (the male wing) and the rapid attenuation rate of particle velocity produce a spatially divergent sound field with highly variable magnitude. Also, male and female** *D. melanogaster* **are not usually stationary during courtship, resulting in a variable directionality of the acoustic stimulus. Using both particle image velocimetry and laser Doppler vibrometry, we examined the stimulus flow around the head of** *D. melanogaster* **to identify the actual geometry of the acoustic input to the antennae and its directional response. We reveal that the stimulus changes in both magnitude and direction as a function of its angle of incidence. Remarkably, directionality is substantial, with inter-antennal velocity differences of 25 dB at 140 Hz. For an organism whose auditory receivers are separated by only 660±51 μm (mean ± s.d.), this inter-antennal velocity difference is far greater than differences in intensity observed between tympanal ears for organisms of similar scale. Further, the mechanical sensitivity of the antennae changes as a function of the angle of incidence of the acoustic stimulus, with peak responses along axes at 45 and 315 deg relative to the longitudinal body axis. This work indicates not only that the flies are able to detect differential cues in signal direction, but also that the male song structure may not be the sole determinant of mating success; his spatial positioning is also crucial to female sound reception and therefore also perhaps to her decision making.**

INTRODUCTION

Animals have evolved many solutions to the problem of locating a sound source, often resulting in far greater accuracy than humans can resolve (see Popper and Fay, 2005). The localisation of a sound source is especially non-trivial for organisms whose small size leaves them subject to non-diffractive conditions, as is the case in many insect species. Hearing organs of insects can be divided into two types: tympanal and flagellar ears. Research has elucidated ingenious mechanisms tympanal insects have evolved to resolve a sound source (see Michelsen et al., 1994; Robert, 2005; Robert et al., 1996); however, empirical work to address directional sensitivity in flagellar, hair-like particle velocity receivers has received far less attention (but see Belton, 1974).

The particle velocity component of a sound wave, quantified by the magnitude and direction of the harmonic oscillations of the particles within a fluid, is detected by many organisms through the displacement of arrays of flagellar receivers, for example, the trichobothria on spiders (Barth, 2004) and cilia on cricket cerci (Shimozawa et al., 2003), or indeed bilateral flagellar ears as found in mosquitoes (Clements, 1999) and fruit flies such as *Drosophila* (Ewing, 1978; Manning, 1967). *Drosophila melanogaster* use bilateral antisymmetric antennae to receive the particle velocity component of an acoustic stimulus (Ewing, 1978; Göpfert and Robert, 2001; Göpfert and Robert, 2002; Manning, 1967). Because of the vectorial nature of the acoustic stimulus, these sensors are considered to be inherently directional. Also, it has been assumed

that the directionality of the signal remains constant between the source and the receiver. However, the presence of an object in a flow, be it a receiver or the organism itself, can change the amplitude and direction of the signal as viscous forces become dominant in a layer around the object (Casas and Dangles, 2010; Schlichting, 1979).

The effects due to the presence of such boundary layers are usually a well-known phenomenon in fluid dynamics and have been studied in biological systems such as swimming (Anderson et al., 2001; Nauen and Lauder, 2001), olfaction (Cox, 2008; Koehl, 2006) and fluid sensing in both air and water (for a review, see Casas and Dangles, 2010). However, the biological contexts in which boundary layer effects are considered usually concern bulk air flow and sensing by arrays of hairs. The reception of acoustic particle velocity depends upon fluid flow, and yet to date, little empirical work has examined the effect of the body of the organism on acoustic signal transmission (Dangles et al., 2008). Instead, it is assumed that the signal at the output, be that sound from a natural source or from a loudspeaker in an experimental setup, remains unchanged despite great increases in viscous forces as the signal approaches the animal.

Acoustic communication is known to be important in *Drosophila* courtship, in which males vibrate an outstretched wing to produce a species-specific song (Ewing and Bennet-Clark, 1968; Rybak et al., 2002; Shorey, 1962). Courtship takes place in the acoustic near-field, where the small size of the dipole sound source (the male
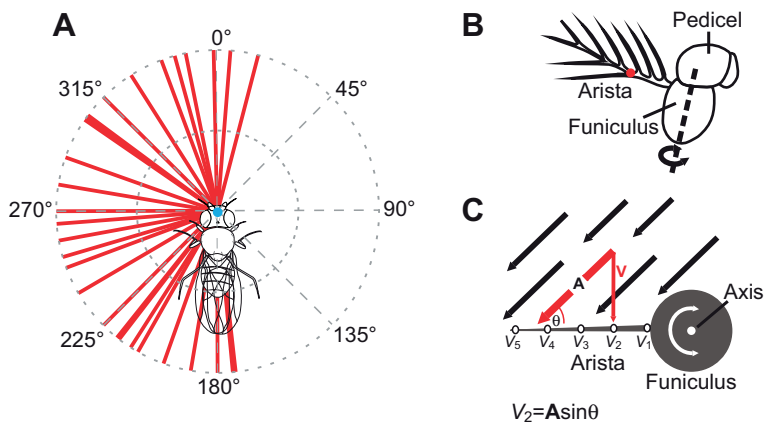
Fig. 1. Particle image velocimetry (PIV) and laser Doppler vibrometry (LDV) measurements of *Drosophila melanogaster* antennae. (A) Red lines show the direction of the stimulus (θ_s), with a centre of rotation between the two antennae (blue circle). (B) Position of LDV measurement on the *D. melanogaster* antenna (red circle) and the rotation of the funiculus. Both the funiculus and the arista rotate about a central axis (dashed line) in response to acoustic stimuli. (C) The values of velocity extracted from the flow were the component perpendicular to the preferred plane of rotational motion of the arista. It is the force perpendicular to the arista length that will generate torque to rotate the funiculus about its axis (semi-circular arrow). Velocity was extracted at five points along the length of the arista (V_1 to V_5) using the equation $V_n = \mathbf{A}_n \sin\theta_n$, where $\mathbf{A}_n$ is the vector of the sound stimulus and θ_n is the vector's direction angle.

wing) and the rapid attenuation rate of particle velocity are expected to produce a highly divergent and localised sound field. To add to this, male *D. melanogaster* are rarely stationary during courtship and therefore the directionality of the stimulus is undoubtedly highly variable. As their antennae have a preferred axis of rotation (Göpfert and Robert, 2001), acoustic sensitivity can potentially be reduced or indeed enhanced depending on the incident stimulus angle. For a tympanal organism of the same size as *D. melanogaster*, the small distance between auditory receivers and the low frequency of sound (typically <300 Hz) received would fail to generate diffraction, leading to inter-aural intensity differences too small to be a reliable cue in sound-source localisation without amplification. However, because of the inherently directional stimulus and boundary effects, the flagellar particle velocity receivers of *D. melanogaster* may well be subject to comparatively large intensity differences.

Here, we use *D. melanogaster* to investigate how particle velocity is modified by the presence of the animal in the sound field and whether and how this affects the subsequent vibrations in their antennae. This study specifically investigates the geometry of the incident particle velocity field in the presence of the fly, mapping the stimulus present at the position of the aristae and measuring the output vibration of the antennae. Knowledge of boundary effects around idealised objects such as a cylinder (Steinmann et al., 2006) would suggest that stimulus amplitude at the receiver should be highly dependent upon stimulus angle. Here, particle image velocimetry (PIV) and laser Doppler vibrometry (LDV) are employed to visualise the flow around the fly head and to measure the nanoscale vibrations generated at the antennae, respectively. We show a change in both the magnitude and direction of the acoustic flow as the signal approaches the animal, variations that are also reflected in the vibrations of the antennal ears. How the flow translates to vibration in the antennae is also examined at different incident angles around the head of the fly. To our knowledge this is the first study to investigate acoustic flows sensed by bilateral flagellar ears in auditory communication.

MATERIALS AND METHODS
Fly strains and maintenance

Drosophila melanogaster Meigen 1830 of the Oregon R strain (stock no. 4269; Bloomington *Drosophila* Stock Center, Bloomington, IN, USA) were maintained on instant fly medium (Carolina Biological Supply Co., Burlington, NC, USA) at 25°C. Female flies were collected and measured 3 days after eclosion.

Acoustic flow measurement

The oscillatory flow around the head of female *D. melanogaster* was measured using PIV. To prepare each fly for measurement, the wings and legs were surgically removed under CO_2 anaesthesia and attached ventrally to a carbon-fibre pin (0.5 mm diameter) using liquid latex. The head, proboscis, scape and pedicel were immobilised using small amounts of latex, by gluing the scape and pedicel to the head and the head to the thorax. A magnified photograph of the fly's head was taken using a PCO Pixelfly double shutter camera (PCO, Kelheim, Germany) mounted onto a Leica MZ125 stereomicroscope (Leica Microsystems, Wetzlar, Germany). After obtaining a clear picture of the aristae position, the aristae were surgically removed. The fly was then allowed to recover from anaesthesia before measurement.

The fly was positioned centrally within a Perspex box (11×11×11 cm) fixed to a turntable. One wall of the Perspex box was composed of a loudspeaker (Visaton FR 108 OHM; Visaton, Haan, Germany) through which a 140 Hz sinusoidal stimulus was provided at 112 dB sound velocity level (SVL; $0\,\text{dB} = 5 \times 10^{-8}\,\text{m s}^{-1}$; $21.5\,\text{mm s}^{-1}$) using a function generator (TTi TG230; Thurlby Thandar Instruments, Huntingdon, Cambridge, UK). SVL was measured using a pressure gradient microphone (Knowles NR-23158-000; Knowles, Itasca, IL, USA) at the position of the head. The signal was recorded *via* a custom-built amplifier modified from that used in Bennet-Clark (Bennet-Clark, 1984) using a USB data acquisition card (NI USB 6009; National Instruments, Austin, TX, USA) and LabView (Version 8.6; National Instruments). The amplitude and stimulus characteristics chosen were within the biologically relevant range of *D. melanogaster* song (Ewing and Bennet-Clark, 1968; Rybak et al., 2002; Tauber and Eberl, 2003; von Schilcher, 1976a; von Schilcher, 1976b). The signal was monitored throughout measurements by positioning the microphone 2.5 cm behind the measured object (fly or cylinder). It was placed at this distance to prevent shadows in the PIV illumination field and disturbance to the flow of interest. Measurements were taken at points sampled from 180 deg with the fly rotated about a central point between the two aristae, where 0 deg corresponds to a flow incident to the front of the head and 270 deg corresponds to a flow incident to the left side of the head as observed from above (Fig. 1A). The range of angles measured was constrained by the shadow of the fly in the laser sheet used to illuminate particles.

The air inside the Perspex box was seeded with 0.2 µm oil droplets (di-ethyl-hexyl-sebacate) using an aerosol generator (Topas ATM 225; Topas, Dresden, Germany). The flow was illuminated using a PIV pulsed laser system (NewWave Research Solo PIV 2, 532 nm, 30 mJ, Nd:YAG, dual-pulsed; Dantec Dynamics, Skovlunde, Denmark). The laser sheet (width=17 mm, thickness at focus point=50 µm) was operated at low power (3 mJ at 532 nm
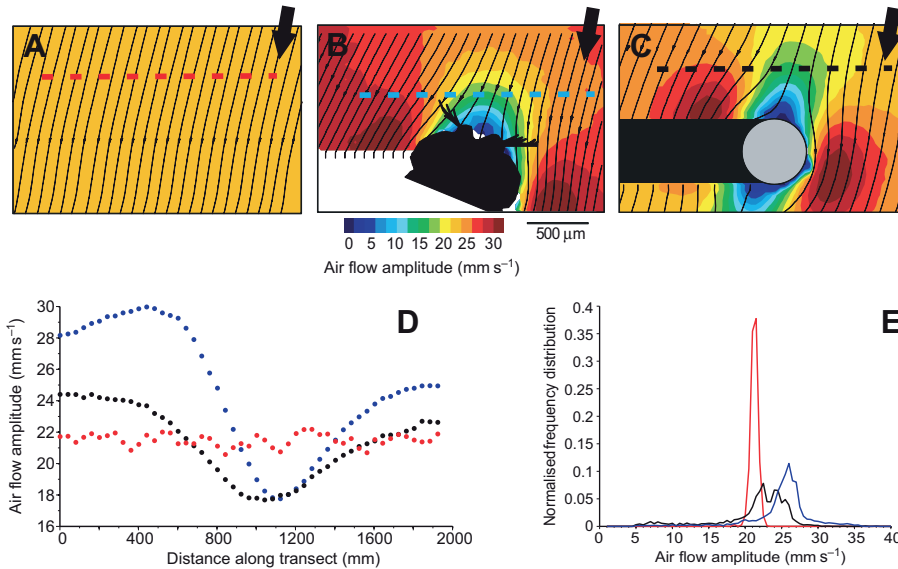
Fig. 2. Acoustic flow patterns (A) in free-field conditions, (B) around the head of a fly and (C) around a cylinder. Streamlines show the direction of flow. The grey circle in C depicts a cross-section of the cylinder; the black area indicates shadow, where no measurement is possible. Large black arrows indicate the direction of flow as delivered by loudspeaker. (D) Velocity profile extracted along the dashed transect lines shown in A–C. Colours correspond to transect colours in A–C. (E) Frequency distribution of flow amplitudes in free-field conditions (red), around the fly head (blue) and around a cylinder (black).

wavelength) with a pulse duration of 4+1 ns. A target area was imaged onto the charge-coupled device (CCD) array of a digital camera (1312×1024 pixels; PCO Pixelfly double shutter) using a stereomicroscope (Leica MZ125) with a 3580×2630 μm field of view. Because of the information contained in the grey-level values captured by CCD as well as the relatively large number of particles used in the cross-correlation calculations, a particle displacement precision of 0.1 pixels was obtained. Given the entire setup, this translates into a measurable particle displacement of 0.27 μm. We set the time between two pairs of images at 1000 μs to provide a sufficient dynamic range of velocities, giving a velocity precision of 0.27 mm s^{-1}. Setting the far-field flow amplitude to 112 dB SVL (21.5 mm s^{-1}), we obtain a precision level close to 1% of the velocity amplitude.

We used the stroboscopic principle to measure different phases of a 140 Hz sinusoidal flow with a PIV system limited to 20 Hz. As explained previously (Steinmann et al., 2006), it consists of sampling a signal of high frequency at a frequency slightly lower than a sub-multiple of the signal frequency. This technique allows us to estimate the flow phase by inference. The flow velocity fields presented in this article are proportional to the amplitude of the flow velocity, i.e. the difference between the maximum velocity measured at $\omega t=\pi/2$ and the minimum velocity measured at $\omega t=-\pi/2$ (where ω is angular frequency and t is time).

Particle velocities and vector maps were calculated by cross-correlation of image pairs using Flow Manager 4.4 software (Dantec Dynamics) averaged over five images at peak oscillation. From the average flow maps, velocity (V_n) was extracted at five equidistant points along the position and length of the removed arista (V_1 to V_5). This was done for both the left and the right arista on each individual measured at each angle (Fig. 1C). Extracted velocity values quantify the magnitude of velocity acting perpendicular to the long axis of the arista.

Antennal vibration measurements

LDV was used to measure antennal vibration in female *D. melanogaster*. Individual female flies were anaesthetised with CO_2 and their wings and legs were surgically removed. A single fly was attached dorsally to a carbon-fibre pin (0.5 mm diameter) using liquid latex. The head, proboscis, scape and pedicel were immobilised using small amounts of latex by gluing the scape and pedicel to the

head and the head to the thorax. The carbon-fibre pin was attached to a brass rod (length: 50 mm, diameter: 5 mm) controlled by a micromanipulator. Once mounted, flies were allowed to recover from anaesthesia before measurement. Only flies showing the active nonlinear frequency response described in Göpfert and Robert (Göpfert and Robert, 2002) were used in LDV measurements.

A sine tone of 140 Hz was generated using the PSV 300 internal data acquisition board (National Instruments PCI-4451), amplified (Sony TAFE570; Sony, Tokyo, Japan) and played at 112 dB SVL through a loudspeaker (Visaton FR 108 OHM) fixed to a turntable. The fly was positioned central to the turntable, 4.5 cm from the centre of the loudspeaker. The acoustic stimulus was monitored using a pressure gradient microphone (Knowles NR-23158-000) fixed centrally on the turntable 5 mm vertically below the fly. This reference microphone was oriented to be maximally sensitive to the particle velocity. The microphone signal was subsequently amplified using a custom-built amplifier modified from that used in Bennet-Clark (Bennet-Clark, 1984) and recorded using Polytec data acquisition and management workstation software (Polytec PSV 8.6; Polytec, Waldbronn, Germany).

The laser spot (~ 5 μm) was reproducibly focused at the base of the first downward branch of each arista (Fig. 1B) and vibration was measured on one antenna for each female fly ($N=20$) using an LDV system (Polytec PSV 300) fitted with a close-up attachment. The arista is known to move as an inflexible rod across the frequency range examined (100–1500 Hz) (Göpfert and Robert, 2002), allowing the use of single point measurements. Both audio and vibrometry data were subjected to a fast Fourier transform in real time. A rectangular window was used with 20 averages and a bandwidth of 1.6 kHz, resulting in a resolution of 1 Hz. All audio and vibrometry recordings were acquired using PSV 8.6 software (Polytec) and were conducted on a vibration isolation table (TMC 784-443-12R; Technical Manufacturing Corp., Peabody, MA, USA) within an anechoic chamber (IAC series 1204A; internal dimensions–length 4.50 m, width 2.25 m, height 1.98 m; Industrial Acoustics, Bronx, NY, USA).

Once a measurement had been taken, the loudspeaker was rotated around the fly at fixed increments sampled from a 360 deg rotation recording responses at each position. To avoid obstructing the laser with the rotation of the loudspeaker, the fly was rotated 180 deg to measure points between 320 and 50 deg for the left arista
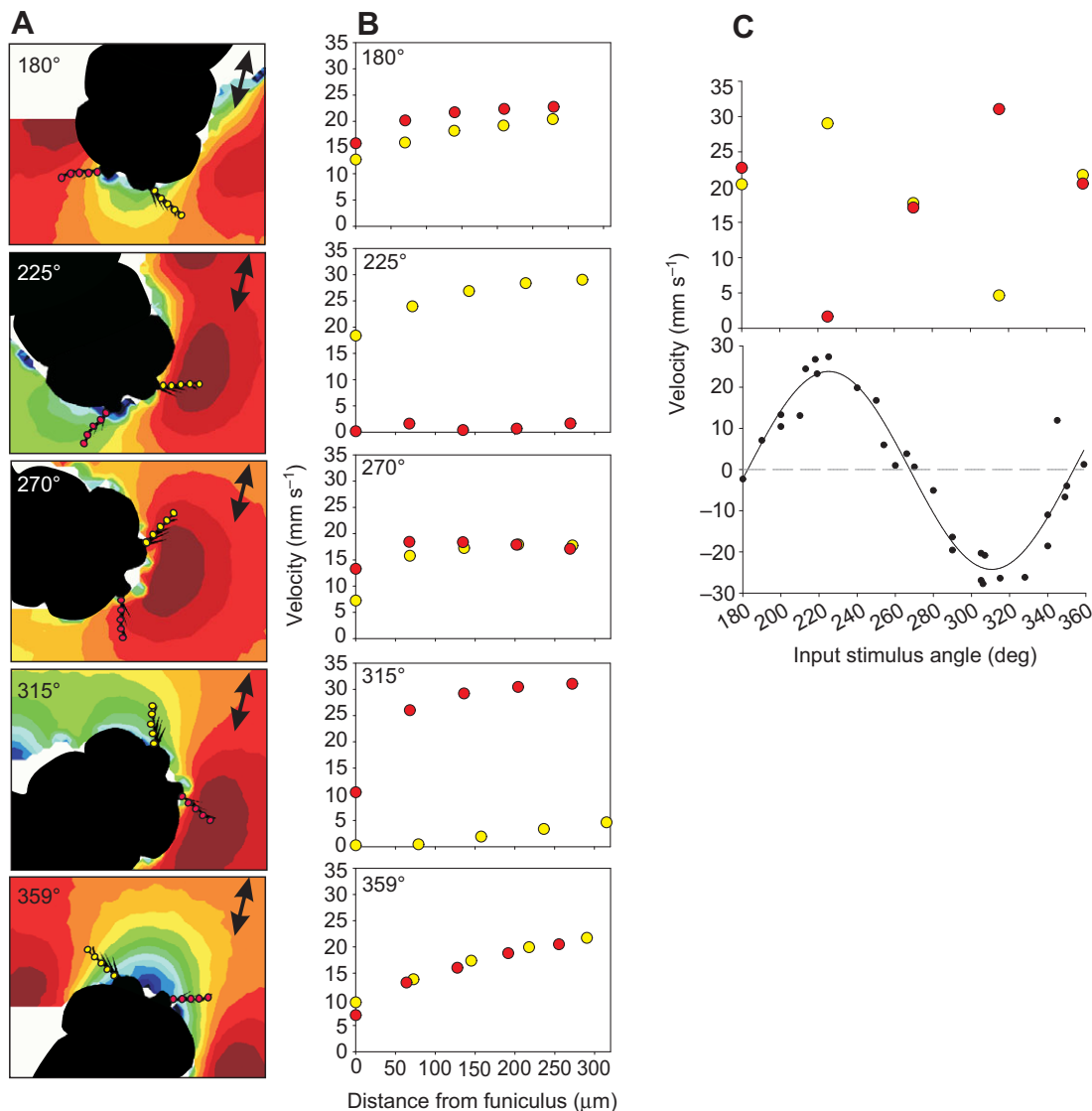
Fig. 3. (A) PIV velocity maps for five stimulus angles around the head of one individual fly. Points along the aristae correspond to positions of velocity extraction (V_1 to V_5; Fig. 1). Large black arrows indicate the direction of the stimulus source. (B) Extracted velocity at five points along each arista for angles corresponding to those in A. Yellow points are the left arista, red points are the right arista. (C) Top: measurements at the arista tip for each of the angles measured on the left and right aristae. Colours are as in B. Bottom: difference in amplitude between the left and right aristae measured in all eight flies at the tip of each arista at each incident angle measured. The line is a sinusoid fit: $y=y_0+\alpha\sin[(2\pi x/b)+c]$ (R^2=0.91).

and point between 40 and 120 deg for the right arista. This could then be compensated for later by inverting the phase measurements of these angles during analysis. The fly was maintained with its head in a central position at all times.

RESULTS
Changes in acoustic flow caused by the presence of *D. melanogaster*

Flow was measured and vector fields were calculated around the heads of eight adult female *D. melanogaster* and around a cylinder. In each case, the acoustic flow in the area examined was modified from a homogeneous vector field of consistent amplitude and directionality (Fig. 2A–C). In some cases the velocity at specific areas around the fly was increased by as much as $15\,\mathrm{mm\,s^{-1}}$ and similarly, certain areas around both the fly and the cylinder were reduced far below the amplitude of free-field flow (Fig. 2D). As predicted, the variability in flow amplitude is greater when a fly or

cylinder is present, with the free-field conditions producing relatively constant amplitude and signal directionality (Fig. 2E). As the flow pattern is highly similar around the fly head and the cylinder in two-dimensional space (Fig. 2C), these effects are likely to be due to the shape of the object, the head itself.

The effect of incident angle on flow amplitude

Dependent on the incident angle of sound, there can be large differences in the amplitude of flow acting on each arista (Fig. 3A). At a stimulus amplitude of 112 dB SVL, the flow velocities at the tip of the two aristae can differ by approximately $30\,\mathrm{mm\,s^{-1}}$, representing an inter-antennal velocity difference (IVD) of 25 dB at incident angles of 225 and 315 deg. This constitutes a 16-fold difference in magnitude of velocity at the position of the two aristae maximally separated by only $660\pm51\,\mu\mathrm{m}$ (N=6) at the arista tips. The pattern of acoustic flow velocity acting at the tip of each arista for different input angles can be fitted with a sinusoid function (Fig. 3C). The position of high and
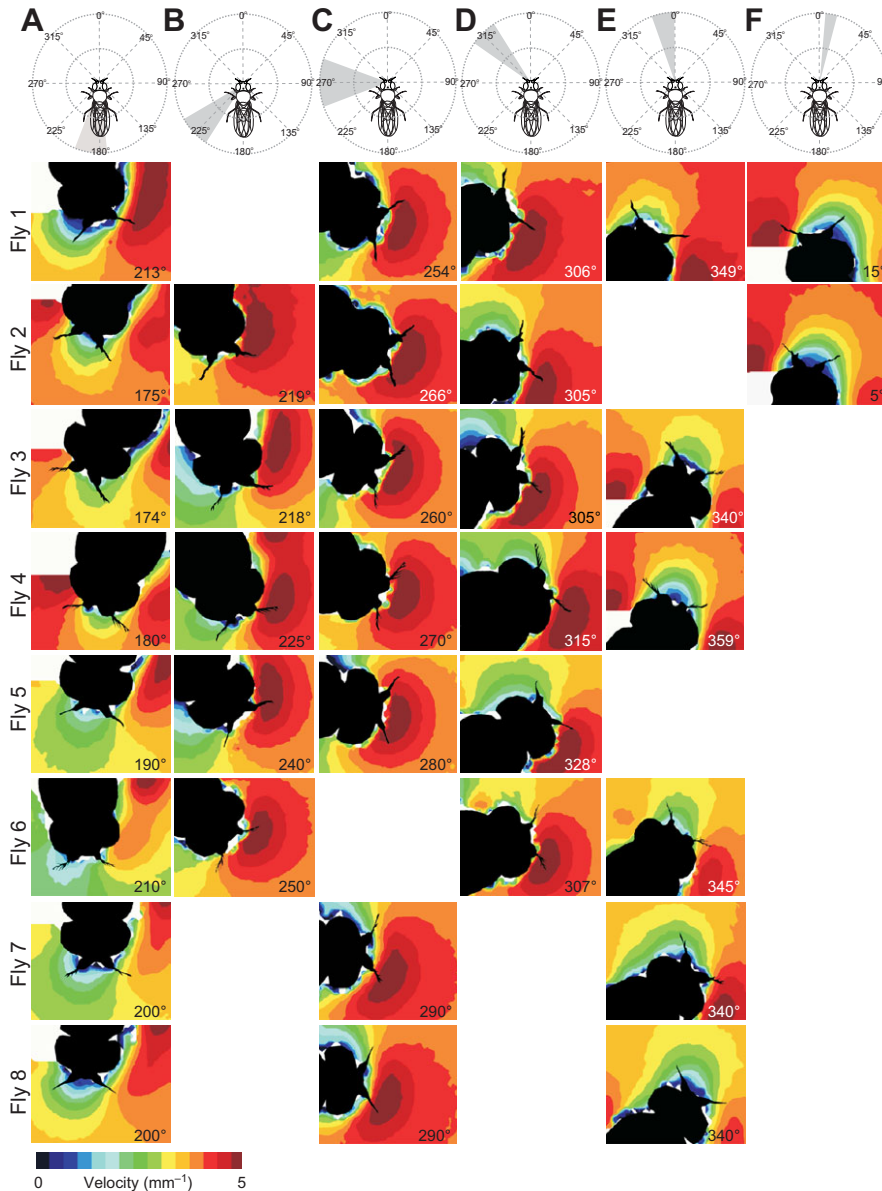
Fig. 4. Oscillatory flow amplitudes around the head of eight female *D. melanogaster*. (A–F) Measurements are grouped by stimulus angle (θ_s), indicated in the grey area of the orientation diagram at the top of each column. Actual stimulus input angles are indicated on each flow map individually. Each row shows measurements taken from a single fly.

low velocity areas appear spatially determined by the stimulus angle. This is consistently seen in all animals measured (Fig. 4). These velocity differences between aristae extracted at the peak of the phase cycle (Figs 3, 4) remain at other phases sampled (Fig. 5), with a lag of approximately $\pi/8$ between the two aristae. The arista receiving lower velocities at the positive phase peak also receives higher velocities at the negative peak of the phase.

Acoustic flow amplitude at aristae

The arista is known to move as a rigid lever without flex (Göpfert and Robert, 2002), displaying the activation of the first vibrational mode of a bar rigidly mounted on a rotary base (Fig. 1B,C). Hence, the forces acting on the entire length of the arista can be considered to generate the torque applied to the funiculus, thus stimulating the mechanosensory cells of Johnston's organ. Calculating absolute forces acting on each arista requires the knowledge of the effective geometry of the branched arista, and the construction of a complicated model. The present paper assumes the arista to be a cylindrical rod protruding from the head of the animal, but in reality it is a branched structure. Branches on a protruding structure can

amplify sensitivity to flow by increasing the surface area available for viscous drag (Schlichting, 1979). For the present purposes, the magnitude of velocity acting perpendicular to the arista length is used and the measurement taken at the position of the arista tip is normalised to the free-field flow (Fig. 1C). Although not quantifying the exact force magnitude along the entire length of the arista, extracting amplitude just at the arista tip gives an initial conservative approximation of forces at the position of the antennae and how they can change.

The data show an axis of symmetry of peak acoustic flow running between 225 and 45 deg for the left arista and between 315 and 135 deg for the right arista (Fig. 6). At these angles, the arista length and its branches are perpendicular to the flow. This allows maximal transfer of force from the flow to generate displacement of the arista.

Acoustic flow direction at the arista

Interestingly, the direction of the particle oscillations next to the arista did not strictly correspond to the direction of propagation defined by the position of the sound source (Fig. 7A). The angle of incidence at the arista was not covariant with the stimulus angle
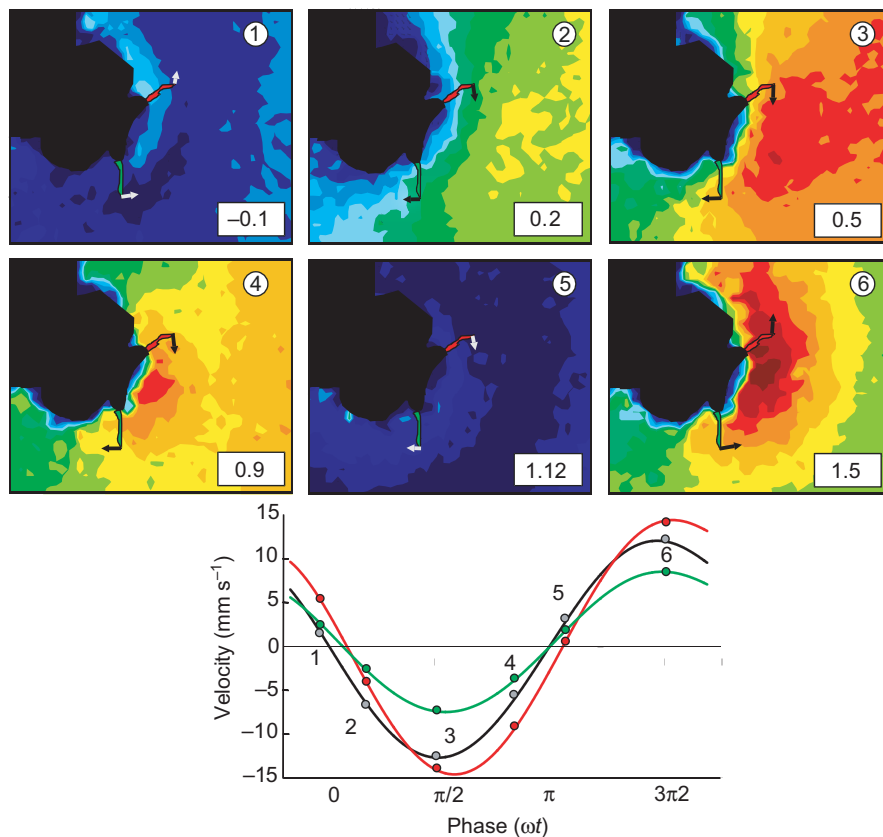
Fig. 5. A snapshot of the flow around *D. melanogaster* head at six points (panels 1–6) through a phase cycle. Arrows indicate the direction of flow. The graph shows the extracted velocity for panels 1–6, where the three curves represent free-field velocity (grey points and black curve), velocity acting on the right arista (green points and curve) and velocity acting on the left arista (red points and curve).

measured at the source of sound. Although generally following a linear trend, the data fit poorly to a linear regression where the angle of stimulus input was the predicted angle of incidence at the antenna (Fig. 7B). Instead, the variation follows a sinusoidal pattern, with maximal differences between input and output angles of 37 deg when the stimulus is presented at approximately 190 and 290 deg for the left arista (Fig. 7C). For the right arista, this is shifted by ca. 60 deg. This shift gives rise to a maximal deviation from prediction close to 250 and 340 deg, instead of 190 and 290 deg for the left arista respectively (Fig. 7C). For the left arista, the difference between the angle of input and incident angle at the arista is smallest where there is peak deviation at the right antenna, approximately 240 and 330 deg. For the right arista, minimal deviation is detected at angles of incidence (200 and 290 deg) similar to those that generate maximal deviations at the left arista.

Antennal vibrations and directional response

The forces in the oscillatory flow must apply a torque through viscous coupling to the arista to produce displacement and stimulation of the mechanosensory cells. For a linear system, the pattern of vibration is expected to follow the peaks and troughs observed in the acoustic flow field. A deviation from this pattern is expected if the active mechanics of the antennae is involved. Measurements taken at 112 dB SVL reveal similar directional patterns, when analysed using cross-correlation, with strong correlations between PIV and LDV measurements in both the left and right arista (left: R^2=0.99, lag=0 deg; right: R^2=0.95, lag=5.7 deg).

There is a maximal difference between the vibration velocity of the left and right aristae at 45, 135, 225 and 315 deg and a minimal difference at 0, 90, 180 and 270 deg as measured by LDV. As the antennae actively amplify quiet stimuli, the antennal vibration does

not fall as low as the acoustic flow measured using PIV (Fig. 8). Instead, the difference in vibration velocity between the two antennae is slightly less than the 25 dB difference in velocity applied to the antennae. However, further investigation and comparison with auditory mutants with a linear antennal response are needed to confirm that it is indeed the active contributions of the mechanosensory cells that are reducing the mechanical IVD of the antennae. Nonetheless, dependent upon the angle of incidence, with
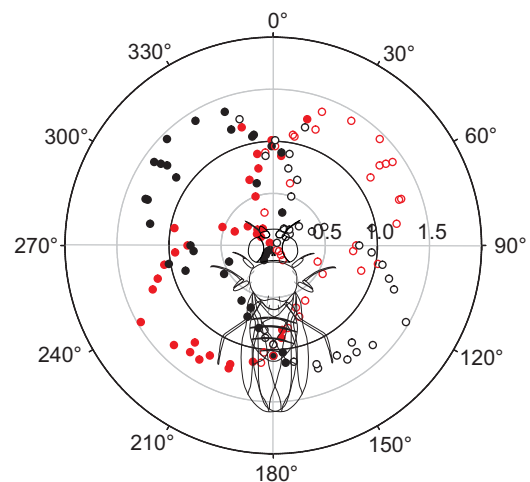

Fig. 6. PIV measurements of oscillatory flow around *D. melanogaster*. Polar plot of acoustic flow amplitude (plot radius) at the arista tip normalised to the mean free-field reference amplitude (21.5 mm s^{-1}; units mm s^{-1}/mm s^{-1}). Solid circles are values measured using PIV (red, left arista; black, right arista); open circles are mirrored measurements assuming symmetry of response to illustrate amplitudes around the full 360 deg.
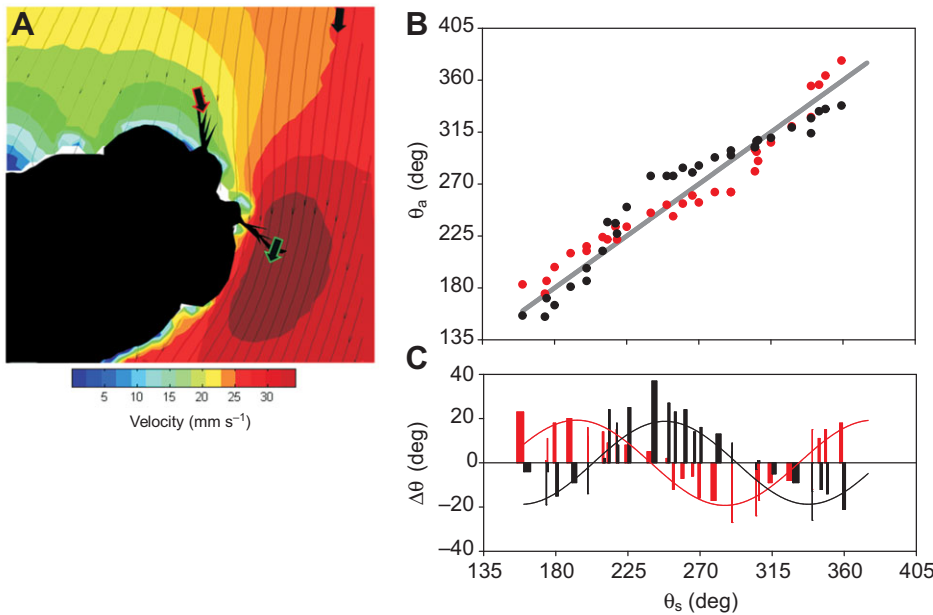
Fig. 7. (A) Streamlines of acoustic flow around the head of *D. melanogaster*. Measurement from an individual fly at a stimulus angle (θ_s) of 225 deg. Arrows in A indicate direction of flow. (B) Linear fit between θ_s and the angle of incidence at the arista (θ_a). Black points, right arista; red points, left arista. The grey line is a regression highlighting deviations in actual input angle at the arista and expected input angle if no change in direction was caused (i.e. the input angle and the actual angle at the arista are the same). (C) Residuals of the difference between θ_s and θ_a ($\theta_s-\theta_a=\Delta\theta$). Colours are as in B. Lines are fits given by a three-parameter sine function $\{y=\alpha\sin[(2\pi x/b) + c]\}$.

the 140 Hz stimulus at 112 dB SVL there is still a considerable mechanical IVD of 15 dB over an angle of incidence range of just 90 deg and spatial separation of just 660±51 µm (*N*=6). Peak amplitude of vibration for the left arista corresponds to stimulus angles of 45 and 225 deg with a minimal stimulation of 90 deg after each peak; peak amplitude of vibration in the right arista occurred at 125 and 290 deg (Fig. 8). The LDV data are inherently more variable than the PIV data because of the ease of aligning the fly precisely in the flow in the latter and the relatively more approximate alignment with LDV, as acoustic flow cannot be visualised and the left and right aristae cannot be measured simultaneously.

DISCUSSION

The presence of the fly in the oscillatory flow modifies both the magnitude and the direction of the signal as it approaches the position of the antennae through boundary effects. At the frequency and amplitude tested here (140 Hz, 112 dB SVL) the antennae are stimulated by the acoustic flow differentially in an angle-dependent manner, eliciting substantial IVDs. In contrast to the minute inter-aural intensity differences experienced in tympanal organisms (see Popper and Fay, 2005), the IVD of 25 dB in *D. melanogaster*, an organism with a head diameter of ~700 µm, is extremely large.

Acoustic flow around *D. melanogaster*

As *D. melanogaster* lives at a scale dominated by viscous forces, the antennae may be expected to have evolved reception mechanisms operating with some degree of efficiency in such viscous regimes. The stimuli should also have evolved to optimise the transmission of information as efficiently as possible in these conditions. However, it is still not clear what information within song a female uses to discriminate between males. Previous work suggests that song frequency is not important to female *D. melanogaster* (Rybak et al., 2002; Talyn and Dowse, 2004) and that timing of pulses is important in species recognition (Bennet-Clark and Ewing, 1969; Talyn and Dowse, 2004). However, the proximate mechanisms used in mate discrimination are not fully understood.

The coupling of the viscous air flow with the mechanics of its biological receivers has been studied in arrays of filiform hairs and trichobothria (for a review, see Casas and Dangles, 2010). The length of the hairs is known to affect their frequency tuning when stimulated with sinusoidal stimuli (Barth et al., 1993; Shimozawa and Kanou, 1984a; Shimozawa and Kanou, 1984b; Shimozawa et al., 1998). However, Kant and Humphrey (Kant and Humphrey, 2009) emphasise that short hairs should be better than long hairs at responding to a pulse, instead of simply responding preferentially
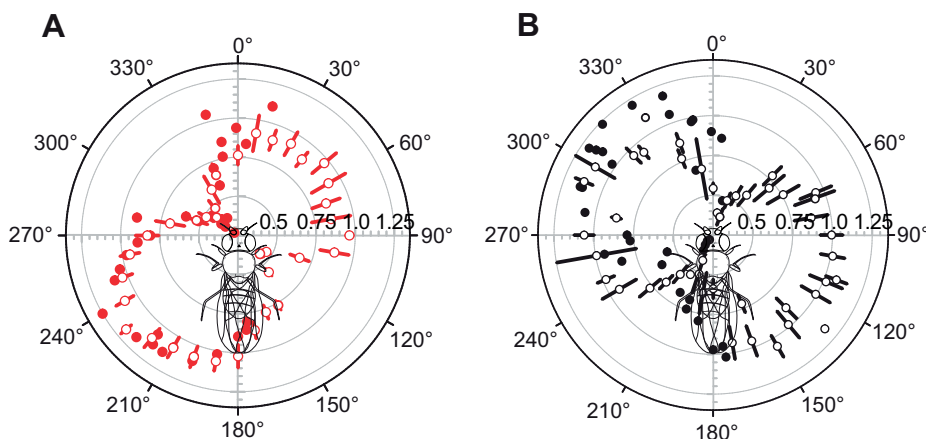

Fig. 8. Antennal mechanical vibration and acoustic flow amplitudes. (A) Mean (±s.e.m.; *N*=5) vibration for the left arista (open circles) measured by LDV, and acoustic flow velocity measured using PIV (filled circles). Acoustic flow velocity is pooled across eight individuals. Data were normalised to allow comparison (dimensionless units). (B) As in A, but for the right arista (*N*=10 for antennal vibration measurements).

to their high resonant frequencies. Interestingly, the pulse component of *D. melanogaster* courtship song, as opposed to the sine element, is deemed to be the component containing key information (Bennet-Clark and Ewing, 1969; von Schilcher, 1976a); this species-specific information is transferred through the inter-pulse interval. It is possible that when the antennae are tuned to high frequencies, as they are with loud stimuli [pulse song at the female antennae can be >100 dB SVL (Jonsson, 2012)], a rapid response of the antennae could convey information through precise timing.

The boundary effects around both the head of the fly and the cylinder generate areas of decreased and increased velocity relative to the stimulus input amplitude (Fig. 2). The size and amplitude of these areas should vary according to the amplitude and frequency of the stimulus applied, as should the thickness of the boundary layer itself. Here, using a stimulus of 140 Hz and 112 dB SVL, the positioning of the aristae allows for the exploitation of this increased velocity along its axis of sensitivity and indeed provides the large IVD amplitude differential between the bilateral receivers. However, establishing the flow patterns and directional mechanical response of the antennae under different stimulus intensities and frequencies requires further investigation, as does the analysis of phase, which may provide further information on the steady state and dynamic mechanisms of directional hearing in *Drosophila*. As the aristae seem to have evolved to detect low power particle velocity stimuli, their positioning in the velocity field is crucial in the detection of male courtship signals. Likewise, the position of flagellar sensors on a cylindrical object can minimise or maximise the boundary effects to effectively enhance signals at the position of the detector. This has potential to inform the design of technological miniature near-field sensors.

Directional sensitivity

The antennal particle velocity receiver in *D. melanogaster* is restricted in rotating about a single central axis (Göpfert and Robert, 2001; Göpfert and Robert, 2002). The structure of many other particle velocity receivers, most notably the antennae in mosquitoes (Clements, 1999), is flagellar and omnidirectional, presumably being deflected in response to the maximum velocity vector. This allows a conceptually simple determination of signal directionality: whichever way the antennae move conveys the source of the sound, incorporating boundary effects. With *D. melanogaster* and perhaps many other dipterans (see Robert and Göpfert, 2002), this inherent directional response of the antenna is removed by restricting the motion of the antenna to be maximally sensitive to forces perpendicular to the arista length. In an animal that uses acoustic communication, the removal of this inherent directional sensitivity of the receiver seems counterintuitive. However, on closer examination, directional sensitivity is maintained in this receiver through angle-dependent differential stimulation of the antennae.

The perception of signal directionality between organisms with tympanal ears and those with flagellar receivers is fundamentally different. As a scalar quantity, pressure has no inherent directionality. In effect, the orientation of a pure pressure receiver in the sound field does not affect its directional sensitivity; with a constant magnitude of sound pressure, and absence of diffractive effects, the receiver detects the same quantity. Directional information can then be extracted by comparing time or intensity cues between bilateral receivers. These cues can be diminishingly small, and indeed require amplifying to be detectable at the neuronal level [see Robert (Robert, 2005) and references therein for reviews]. For *D. melanogaster*, the reception of particle velocity also involves intensity and time cues at each antenna. It is shown here that IVDs are considerable,

amounting to a 25 dB difference between antennae separated at most by 660±51 μm (*N*=6; Fig. 3).

The antisymmetric antennae of *D. melanogaster* conceivably increase this difference mechanically by limiting the angles capable of generating maximal rotational displacements. In their single axis of rotation in response to stimuli from all directions, however, the *D. melanogaster* antennae effectively remove directional sensitivity. In mosquitoes, also using flagellar antennae to receive particle velocity, antennae are able to move in all directions and their motion should correspond with the velocity vector in the local sound field.

For tympanal organisms, proximity to the sound source, within free-field conditions at least, usually correlates well with intensity. Here, with *D. melanogaster*, proximity to the sound source does not necessarily equate to greater amplitude. Orientation is important, as the ipsilateral receiver will be minimally stimulated at certain angles, whereas the antenna on the contralateral side will show a peak vibration magnitude (Fig. 8). We may speculate from this that the favoured singing positions for a male should correspond to peak sensitivities of the antennae (45, 135, 225 and 315 deg; Fig. 8), but further behavioural evidence for this is required.

These large differences between what the two antennae receive may be significant when it comes to acoustic communication in courtship. Males are rarely stationary throughout a bout of courtship song, and likewise the female is often trying to walk away. Furthermore, with the inherent directionality of particle velocity and the proximity of the male to the female, the geometry of sound radiation from the vibrating wing is likely to be highly divergent. From the theoretical dipole of a singing male wing, attenuation is expected to be high, with amplitude decreasing by a relationship of $1/r^3$, where *r* is the distance from the source (Bennet-Clark, 1984), and divergent radiation patterns close to a sound source mean that large fluctuations in amplitude are a factor that organisms using near-field particle velocity may have evolved mechanisms to utilise. The antennae themselves do not simply receive stimuli passively, but behave in a nonlinear, active manner (Göpfert and Robert, 2001; Göpfert and Robert, 2002). Indeed, quiet stimuli are amplified through active input by the mechanosensory neurons themselves (Göpfert and Albert, 2006; Göpfert and Robert, 2003b). Moreover, the resonant characteristics of the antennae vary with sound intensity (Göpfert and Robert, 2002). In effect, along a continuum, low intensities generate lower resonant frequencies than higher intensities through an active process, effectively altering the stiffness of the auditory receiver (Göpfert and Robert, 2001; Göpfert and Robert, 2002; Göpfert and Robert, 2003a; Göpfert and Robert, 2003b). Because of this amplitude-dependent antennal response, the position of the male as he sings relative to the female should be crucial in determining the signal that she receives. As yet, the importance of male singing position to mating success has not been quantified. In fact, little is known about the geometry of sound radiation emitted from a male wing. Bennet-Clark (Bennet-Clark, 1971) calculated the theoretical amplitude of the song; however, there has been little attempt to examine empirically the absolute amplitudes around a wing or the geometry of emission. When the geometry of the wing is factored in to the detection of direction of a signal, it may well be that the effects noted in the present study are amplified (i.e. large IVD, deviation from the initial flow direction and the key directions for antennal sensitivity).

The nonlinear mechanics of the antennae imply that amplitude is important in *Drosophila* hearing. In this study, following the requirements of the PIV technique, we used amplitudes at the high end but within the biologically relevant range for *D. melanogaster* (Bennet-Clark, 1971) of 112 dB SVL. Investigations into the

directional antennal response using a range of stimulus amplitudes may reveal active enhancement of signal detection in an angle-dependent manner. If so, it is possible that an increase in sensitivity to low amplitudes is required to maintain a differential in amplitude between the two antennae when the stimulus at one antenna is small. Integrating the input from two receivers would allow more accurate directional detection and determination of distance than relying on the input of a single receiver. Therefore, if the range of angles where stimulus levels fall below the hearing threshold is large, a receiver without amplification at low amplitudes would have less information about the location of the sound source. As amplitude decreases, the antenna not only becomes mechanically more sensitive to the stimulus, but it also shifts its frequency tuning (Göpfert and Robert, 2002). It is possible that where the antenna is subject to a non-linear regime, a change in stimulus angle can correspond not only to a perceived change in amplitude, but also a shift in the frequencies preferentially detected. From the present work using a sine stimulus at a single frequency it is not possible to determine the effect of stimulus angle on antennal spectral tuning. Future studies could explore whether males need to get their singing position right to be heard, as the placement of the male may affect the frequency tuning of the female's ears, and hence the detectability of their courtship signal.

Conclusions

The acoustic cues used in *D. melanogaster* courtship have been studied for nearly 50 years, and yet it is still not clear what cues the female uses to discriminate between males and accept or reject mating attempts. Perhaps focusing on the structure of the song alone has been simplifying the situation. From this study we now know that as males move around females during courtship, the female antennae are responding with extreme directionality and possibly large changes in tuning. One consequence is that courtship in *Drosophila* is not as simple as it seems, and that the relative position of the protagonists is as important as the structure of the song itself.

REFERENCES

Anderson, E. J., McGillis, W. R. and Grosenbaugh, M. A. (2001). The boundary layer of swimming fish. *J. Exp. Biol.* **204**, 81-102.

Barth, F. G. (2004). Spider mechanoreceptors. *Curr. Opin. Neurobiol.* **14**, 415-422.

Barth, F. G., Wastl, U., Humphrey, J. A. C. and Devarakonda, R. (1993). Dynamics of arthropod filiform hairs. 2. Mechanical-properties of spider trichobothria (*Cupiennius salei* Keys). *Philos. Trans. R. Soc. Lond. B* **340**, 445-461.

Belton, P. (1974). An analysis of direction finding in male mosquitoes. In *Experimental Analysis of Insect Behaviour* (ed. L. B. Brown), pp. 139-148. New York: Springer.

Bennet-Clark, H. C. (1971). Acoustics of insect song. *Nature* **234**, 255-259.

Bennet-Clark, H. C. (1984). A particle velocity microphone for the song of small insects and other acoustic measurements. *J. Exp. Biol.* **108**, 459-463.

Bennet-Clark, H. C. and Ewing, A. W. (1969). Pulse interval as a critical parameter in courtship song of *Drosophila melanogaster*. *Anim. Behav.* **17**, 755-759.

Casas, J. and Dangles, O. (2010). Physical ecology of fluid flow sensing in arthropods. *Annu. Rev. Entomol.* **55**, 505-520.

Clements, A. N. (1999). *The Biology of Mosquitoes: Sensory Reception and Behaviour*. New York: CABI.

Cox, J. P. L. (2008). Hydrodynamic aspects of fish olfaction. *J. R. Soc. Interface* **5**, 575-593.

Dangles, O., Steinmann, T., Pierre, D., Vannier, F. and Casas, J. (2008). Relative contributions of organ shape and receptor arrangement to the design of cricket's cercal system. *J. Comp. Physiol. A* **194**, 653-663.

Ewing, A. W. (1978). Antenna of *Drosophila* as a love song receptor. *Physiol. Entomol.* **3**, 33-36.

Ewing, A. W. and Bennet-Clark, H. C. (1968). The courtship songs of *Drosophila*. *Behaviour* **31**, 288-301.

Göpfert, M. C. and Albert, J. T. (2006). Mechanical energy contributed by motile neurons in the *Drosophila* ear. In *Auditory Mechanisms: Processes and Models* (ed. A. L. Nuttall, T. Ren, P. Gillespie, K. Grosh and E. de Boer), pp. 489-495. Singapore: World Scientific.

Göpfert, M. C. and Robert, D. (2001). Biomechanics. Turning the key on *Drosophila* audition. *Nature* **411**, 908.

Göpfert, M. C. and Robert, D. (2002). The mechanical basis of *Drosophila* audition. *J. Exp. Biol.* **205**, 1199-1208.

Göpfert, M. C. and Robert, D. (2003a). Micromechanics of *Drosophila* audition. In *Biophysics of the Cochlea: From Molecules to Models* (ed. A. W. Gummer, E. Dalhoff, M. Nowotny and M. P. Scherer), pp. 300-307. Singapore: World Scientific.

Göpfert, M. C. and Robert, D. (2003b). Motion generation by *Drosophila* mechanosensory neurons. *Proc. Natl. Acad. Sci. USA* **100**, 5514-5519.

Jonsson, T. (2012). Analysis of behaviour, acoustics, and communication during courtship in *Drosophila melanogaster*. PhD thesis, University of Bristol.

Kant, R. and Humphrey, J. A. C. (2009). Response of cricket and spider motion-sensing hairs to airflow pulsations. *J. R. Soc. Interface* **6**, 1047-1064.

Koehl, M. A. R. (2006). The fluid mechanics of arthropod sniffing in turbulent odor plumes. *Chem. Senses* **31**, 93-105.

Manning, A. (1967). Antennae and sexual receptivity in *Drosophila melanogaster* females. *Science* **158**, 136-137.

Michelsen, A., Popov, A. V. and Lewis, B. (1994). Physics of directional hearing in the cricket *Gryllus bimaculatus*. *J. Comp. Physiol. A* **175**, 153-164.

Nauen, J. C. and Lauder, G. V. (2001). Locomotion in scombrid fishes: visualization of flow around the caudal peduncle and finlets of the chub mackerel *Scomber japonicus*. *J. Exp. Biol.* **204**, 2251-2263.

Popper, A. N. and Fay, R. R. (2005). *Sound Source Localisation*. New York: Springer.

Robert, D. (2005). Directional hearing in insects. In *Springer Handbook of Auditory Research: Sound Source Localization* (ed. A. N. Popper and R. R. Fay), pp. 6-35. New York: Springer Science and Business Media.

Robert, D. and Göpfert, M. C. (2002). Acoustic sensitivity of fly antennae. *J. Insect Physiol.* **48**, 189-196.

Robert, D., Miles, R. N. and Hoy, R. R. (1996). Directional hearing by mechanical coupling in the parasitoid fly *Ormia ochracea*. *J. Comp. Physiol. A* **179**, 29-44.

Rybak, F., Aubin, T., Moulin, B. and Jallon, J. M. (2002). Acoustic communication in *Drosophila melanogaster* courtship: are pulse- and sine-song frequencies important for courtship success? *Can. J. Zool.* **80**, 987-996.

Schlichting, H. (1979). *Boundary Layer Theory*. New York: McGraw-Hill.

Shimozawa, T. and Kanou, M. (1984a). The aerodynamics and sensory physiology of range fractionation in the cercal filiform sensilla of the cricket *Gryllus bimaculatus*. *J. Comp. Physiol.* **155**, 495-505.

Shimozawa, T. and Kanou, M. (1984b). Varieties of filiform hairs – range fractionation by sensory afferents and cercal interneurons of a cricket. *J. Comp. Physiol.* **155**, 485-493.

Shimozawa, T., Kumagai, T. and Baba, Y. (1998). Structural scaling and functional design of the cercal wind-receptor hairs of cricket. *J. Comp. Physiol. A* **183**, 171-186.

Shimozawa, T., Murakami, J. and Kumagai, T. (2003). Cricket wind receptors: thermal noise for the highest sensitivity known. In *Sensors and Sensing in Biology and Engineering* (ed. F. G. Barth, J. A. C. Humphrey and T. W. Secomb), pp. 145-157. Basel: Birkhäuser.

Shorey, H. H. (1962). Nature of the sound produced by *Drosophila melanogaster* during courtship. *Science* **137**, 677-678.

Steinmann, T., Casas, J., Krijnen, G. and Dangles, O. (2006). Air-flow sensitive hairs: boundary layers in oscillatory flows around arthropod appendages. *J. Exp. Biol.* **209**, 4398-4408.

Talyn, B. C. and Dowse, H. B. (2004). The role of courtship song in sexual selection and species recognition by female *Drosophila melanogaster*. *Anim. Behav.* **68**, 1165-1180.

Tauber, E. and Eberl, D. F. (2003). Acoustic communication in *Drosophila*. *Behav. Processes* **64**, 197-210.

von Schilcher, F. (1976a). The function of pulse song and sine song in the courtship of *Drosophila melanogaster*. *Anim. Behav.* **24**, 622-625.

von Schilcher, F. (1976b). Role of auditory stimuli in courtship of *Drosophila melanogaster*. *Anim. Behav.* **24**, 18-26.